Galectin-3 directs antimicrobial guanylate binding proteins to vacuoles furnished with bacterial secretion systems

Eric M. Feeley[a,1], Danielle M. Pilla-Moffett[a,1], Erin E. Zwack[b], Anthony S. Piro[a], Ryan Finethy[a], Joseph P. Kolb[c], Jennifer Martinez[c], Igor E. Brodsky[b], and Jörn Coers[a,d,2]

[a]Department of Molecular Genetics and Microbiology, Duke University Medical Center, Durham, NC 27710; [b]Department of Pathobiology, School of Veterinary Medicine, University of Pennsylvania, Philadelphia, PA 19104; [c]Immunity, Inflammation, and Disease Laboratory, National Institute of Environmental Health Sciences, National Institutes of Health, Research Triangle Park, NC 27709; and [d]Department of Immunology, Duke University Medical Center, Durham, NC 27710

Edited by Ralph R. Isberg, Howard Hughes Medical Institute/Tufts University School of Medicine, Boston, MA, and approved January 20, 2017 (received for review September 23, 2016)

Many invasive bacteria establish pathogen-containing vacuoles (PVs) as intracellular niches for microbial growth. Immunity to these infections is dependent on the ability of host cells to recognize PVs as targets for host defense. The delivery of several host defense proteins to PVs is controlled by IFN-inducible guanylate binding proteins (GBPs), which themselves dock to PVs through poorly characterized mechanisms. Here, we demonstrate that GBPs detect the presence of bacterial protein secretion systems as "patterns of pathogenesis" associated with PVs. We report that the delivery of GBP2 to *Legionella*-containing vacuoles is dependent on the bacterial Dot/Icm secretion system, whereas the delivery of GBP2 to *Yersinia*-containing vacuoles (YCVs) requires hypersecretion of *Yersinia* translocon proteins. We show that the presence of bacterial secretion systems directs cytosolic carbohydrate-binding protein Galectin-3 to PVs and that the delivery of GBP1 and GBP2 to *Legionella*-containing vacuoles or YCVs is substantially diminished in Galectin-3–deficient cells. Our results illustrate that insertion of bacterial secretion systems into PV membranes stimulates Galectin-3–dependent recruitment of antimicrobial GBPs to PVs as part of a coordinated host defense program.

interferon | guanylate binding proteins | immunity-related GTPase | galectin | ubiquitin

Most pathogenic bacteria remodel the phagosomes that they occupy into vesicles defective for phagolysosomal fusion (1). In addition to blocking lysosomal maturation, pathogens commonly manipulate their surrounding vacuolar compartments in a number of ways to assure nutrient acquisition. To customize phagosomes into beneficial pathogen-containing vacuoles (PVs), intravacuolar bacteria use secretion systems to release effector proteins from the bacterial cytoplasm into the host cell cytosol (1). These secretion systems are essential for bacterial virulence. Some of the structural components of bacterial secretion systems are highly conserved and shared among many distinct bacterial species (2). This conservation is exploited by the innate immune system, which evolved cytosolic pattern recognition receptors (PRRs) that can detect conserved components such as the basal body rod component or the needle protein of type III secretion systems (T3SS) (3). Distinct molecular features of these conserved T3SS structural proteins constitute pathogen-associated molecular patterns (PAMPs) that are directly recognized by host PRRs. In addition to the direct recognition of structural components of bacterial secretion systems, the host is also able to detect the presence of secretion system indirectly by sensing cellular perturbations caused by secreted bacterial effector proteins. These microbe-directed perturbations are often shared among different types of infections and thus constitute conserved "pattern of pathogenesis" (4). For example, some bacterial effectors modify the lipid composition of PVs. As a potential consequence of these lipid modifications, PVs are more likely to rupture when exposed to cytoskeleton motor-dependent mechanical forces (5, 6). Although pathogens such as *Legionella pneumophila* or *Salmonella enterica* secrete effectors to counteract destabilizing effects of membrane manipulations to maintain the PV as a replicative niche (7–9), subsets of *Legionella*-containing vacuoles (LCVs) or *Salmonella*-containing vacuoles (SCVs) nonetheless fail to maintain their membrane integrity (7, 10).

Vacuolar instability is recognized by host β-*gal*–binding proteins of the Galectin family (11). Galectins are nucleocytoplasmic proteins that can also be exported from cells through a poorly defined unconventional secretion pathway. Extracellular Galectins can bind directly to bacteria, mediate bacteriostatic or bactericidal effects, and modify inflammatory signaling events (11). More recently, intracellular Galectin-3 was characterized as a sensor of vacuolar rupture that occurs when bacteria such as *Shigella flexneri* actively enter the host cell cytosol (12). Galectin-3 also detects LCVs and SCVs, and Galectin-8 and -9 were also shown to associate with SCVs (7, 10, 13). The association of Galectins with SCVs is largely dependent on host glycans restricted to the vacuolar lumen, indicating that SCVs display

Significance

To combat infections with bacterial pathogens that reside and replicate inside specialized intracellular vacuoles, the innate immune system must be able to distinguish these pathogen-containing vacuoles (PVs) from endogenous vesicles. Here, we demonstrate that the host can detect the presence of bacterial secretion systems as hallmarks of PVs. The insertion of bacterial protein secretion pores destabilizes vesicular membranes, allowing host carbohydrate-binding proteins to access the sugar-decorated luminal side of vacuolar membranes. We show that a specific carbohydrate-binding protein recruits members of a family of antimicrobial GTPases to PVs. Our findings reveal how host cells deliver antimicrobial defenses specifically to intracellular vesicles occupied by pathogens.

Author contributions: E.M.F., D.M.P.-M., and J.C. designed research; E.M.F., D.M.P.-M., E.E.Z., A.S.P., and R.F. performed research; E.M.F., D.M.P.-M., E.E.Z., A.S.P., R.F., J.P.K., J.M., and I.E.B. contributed new reagents/analytic tools; E.M.F., D.M.P.-M., and J.C. analyzed data; E.M.F. and J.C. wrote the paper; and I.E.B. and J.C. supervised the project.

The authors declare no conflict of interest.

This article is a PNAS Direct Submission.

Freely available online through the PNAS open access option.

[1]E.M.F. and D.M.P.-M. contributed equally to this work.

[2]To whom correspondence should be addressed. Email: jorn.coers@duke.edu.

This article contains supporting information online at www.pnas.org/lookup/suppl/doi:10.1073/pnas.1615771114/-/DCSupplemental.

membrane lesions that can be recognized by the host. Galectin-8 was shown to interact with the autophagy adaptor protein NDP52 and to promote the delivery of NDP52 to SCVs, which results in diminished intracellular bacterial survival (10). The functional consequences of recruiting Galectin-9 or Galectin-3 to SCVs or other PVs have remained unexplored.

Whereas galectins are constitutively expressed in macrophages and other cell types (11), many cell-intrinsic host defense programs are activated by proinflammatory cytokines, and IFNs in particular (14, 15). IFNs robustly induce the expression of host resistance factors, including immunity-related GTPases (IRGs) and guanylate binding proteins (GBPs) (16, 17). IRGs and GBPs facilitate cell-intrinsic immunity in vitro and host resistance in vivo to a broad spectrum of intracellular pathogens (16). In infected cells, IRGs and GBPs colocalize with intracellular bacterial pathogens residing in the host cell cytosol or within PVs (16, 18), and several studies have suggested functional interactions between members of the IRG and GBP families (18–23). Although IRGs and GBPs can combat intracellular infections cooperatively, mounting evidence suggests that these two protein families also execute unique cellular functions independent of one another (16). For example, IRGs facilitate the delivery of ubiquitin E3 ligases to *Toxoplasma*- and *Chlamydia*-containing vacuoles independent of GBPs (21, 22). GBPs, on the contrary, were reported to control the deposition of the NADPH oxidase NOX2 at *Mycobacterium*-containing phagosomes independent of IRGs (24). These studies broadly characterize IRGs and GBPs as escorts for distinct antimicrobial factors en route to PVs. However, the mechanisms by which IRGs and GBPs detect and bind to PVs remain poorly characterized (25).

We previously demonstrated that IRGs are essential for targeting GBPs to *Toxoplasma*- and *Chlamydia*-containing vacuoles (20, 21). In this study, we describe an IRG-independent pathway by which GBPs are delivered to PVs. We show that Galectin-3 and murine GBP2 (mGBP2) form protein complexes, which associate with vacuoles harboring secretion system-competent *L. pneumophila* or *Yersinia pseudotuberculosis*. We demonstrate that the secretion of translocon proteins by *Y. pseudotuberculosis* is critical for the recruitment of Galectin-3 and mGBP2 to *Yersinia*-containing vacuoles (YCVs). We further describe a functional role for Galectin-3 in the delivery of mGBP2 and mGBP1 to YCVs and LCVs. Our study thus characterizes bacterial secretion apparatuses as PV-associated patterns of pathogenesis that trigger Galectin-3–dependent recruitment of antimicrobial GBPs.

Results

GBPs Associate with LCVs Independent of ATG and IRG Proteins. Members of the GBP and IRG families of IFN-inducible GTPases have been shown to colocalize with several types of PVs (16). To determine whether this extends to LCVs, we first monitored the subcellular localization of ectopically expressed mGBP1, mGBP2, and mGBP7 GFP-fusion proteins in murine RAW 264.7 macrophages. In these and all subsequent experiments, we used flagellin-deficient (*ΔflaA*) *L. pneumophila* strains to prevent the flagellin-dependent activation of the NAIP5-NLRC4 inflammasome and the subsequent pyroptotic cell death (26, 27). We observed that ectopically expressed mGBPs decorated LCVs in RAW 264.7 cells (Fig. 1*A*), as did endogenous mGBP2 in IFN-γ–primed bone marrow-derived macrophages (BMDMs; Fig. 1*B*). Recruitment of mGBP2 to LCVs was detected as early as 20 min postinfection, albeit at low frequency. The frequency of mGBP2-positive LCVs steadily increased over the course of the first 2 h of infection (Fig. 1*C*). LCVs also attracted the IRG proteins Irgb10 and Irgb6 (Fig. 1*D*), thus mimicking observations made for PVs formed by the bacterium *Chlamydia trachomatis* and the protozoan *Toxoplasma gondii* (28, 29). We previously reported that the regulatory IRG proteins Irgm1 and Irgm3 are required for delivery of Irgb10 and Irgb6 to *Chlamydia* and *Toxoplasma* PVs (20). Similar to these previous observations, we found that the recruitment of Irgb10 and Irgb6 to LCVs was greatly diminished in *Irgm1*$^{-/-}$*Irgm3*$^{-/-}$ BMDMs (Fig. 1*D*), suggesting a shared regulatory role for Irgm1 and Irgm3 proteins in the targeting of IRG proteins to LCVs and *Chlamydia* and *Toxoplasma* PVs.

Irgm1 and Irgm3 not only control the subcellular localization of other IRGs but also are essential for the delivery of GBPs to *Chlamydia* and *Toxoplasma* PVs in mouse cells (20, 21). In *Irgm1*$^{-/-}$*Irgm3*$^{-/-}$ BMDMs, mGBP2 mislocalizes to vesicular structures (19), as independently confirmed in the present study (Fig. S1*A*). However, despite this altered staining pattern, mGBP2 associated with LCVs at a comparable frequency in WT and *Irgm1*$^{-/-}$*Irgm3*$^{-/-}$ BMDMs (Fig. 1*E* and Fig. S1*A*). We then proceeded to test additional host factors known to be required for the targeting of GBPs to *Chlamydia* and *Toxoplasma* PVs for their role in the recruitment of mGBP2 to LCVs. One such host factor is the protein ATG5 (30–33), which participates in autophagosome formation and the lipidation of ubiquitin-like ATG8 proteins, including the autophagosomal marker LC3 (34). Although some mGBP2 protein mislocalized to ring-like structures in *Atg5*$^{-/-}$ BMDMs (Fig. S1*A*), we found that ATG5 was not required for the recruitment of mGBP2 to LCVs (Fig. 1*F*). Additionally, we observed that mGBP2 targeting to LCVs was independent of the autophagy proteins Beclin1 and Atg7 (Fig. S1*B*). Together, these data indicate that mGBP2 recruitment to LCVs is mechanistically distinct from its targeting to *Chlamydia* and *Toxoplasma* PVs.

The Presence of Bacterial Secretion Systems Dictates the Recruitment of mGBP2 to LCVs and YCVs. To characterize this newly described IRG- and ATG-independent GBP delivery system, we asked what specific properties of LCVs were recognized by the cell-autonomous immune system to assure the specific targeting of mGBP2 to LCVs. The most simplistic model posited that mGBP2 was indiscriminately recruited to the phagocytic cup or early phagosomes, and as such would target to any internalized cargo. To test this model, we fed live and dead *L. pneumophila* bacteria or latex beads to IFN-γ–primed BMDMs. At 2 h postinfection (hpi), mGBP2 frequently decorated LCVs formed by live bacteria but remained absent from phagosomes containing formalin-fixed or heat-inactivated bacteria or latex beads (Fig. 2*A*). These data demonstrated that mGBP2 was exclusively recruited to vacuoles containing live bacteria. We therefore hypothesized that vacuoles containing live *L. pneumophila* featured a unique PAMP or pattern of pathogenesis that is detected by the host and prompts the deposition of mGBP2 at LCVs.

Common to many bacterial pathogens is the use of bacterial secretion systems to deliver virulence factors across eukaryotic membranes. We therefore hypothesized that the presence of bacterial secretion systems at PVs could constitute a pattern recognizable by host GBPs. *L. pneumophila* extensively remodels its surrounding vacuole through the secretion of bacterial effector proteins by the Dot/Icm type IV secretion system (T4SS), a process that requires the bacterial scaffolding protein dotA (35, 36). We found that vacuoles containing dotA-deficient bacteria remained devoid of mGBP2 (Fig. 2*B*). In macrophages coinfected with Δ*dotA* and WT *L. pneumophila*, mGBP2 exclusively recruited to WT LCVs (Fig. S2). These data demonstrated that the host recognizes the presence of the Dot/Icm T4SS in a phagosome-intrinsic manner, resulting in the deposition of mGBP2 at WT LCVs.

We reasoned that the host could detect PV-associated bacterial secretion systems by two distinct mechanisms: the host could sense the presence of the bacterial secretion apparatus or detect the activity of secreted bacterial effector proteins. To distinguish between these two mechanisms, we tested whether the apparatus of a second bacterial secretion system, the T3SS of *Y. pseudotuberculosis*,

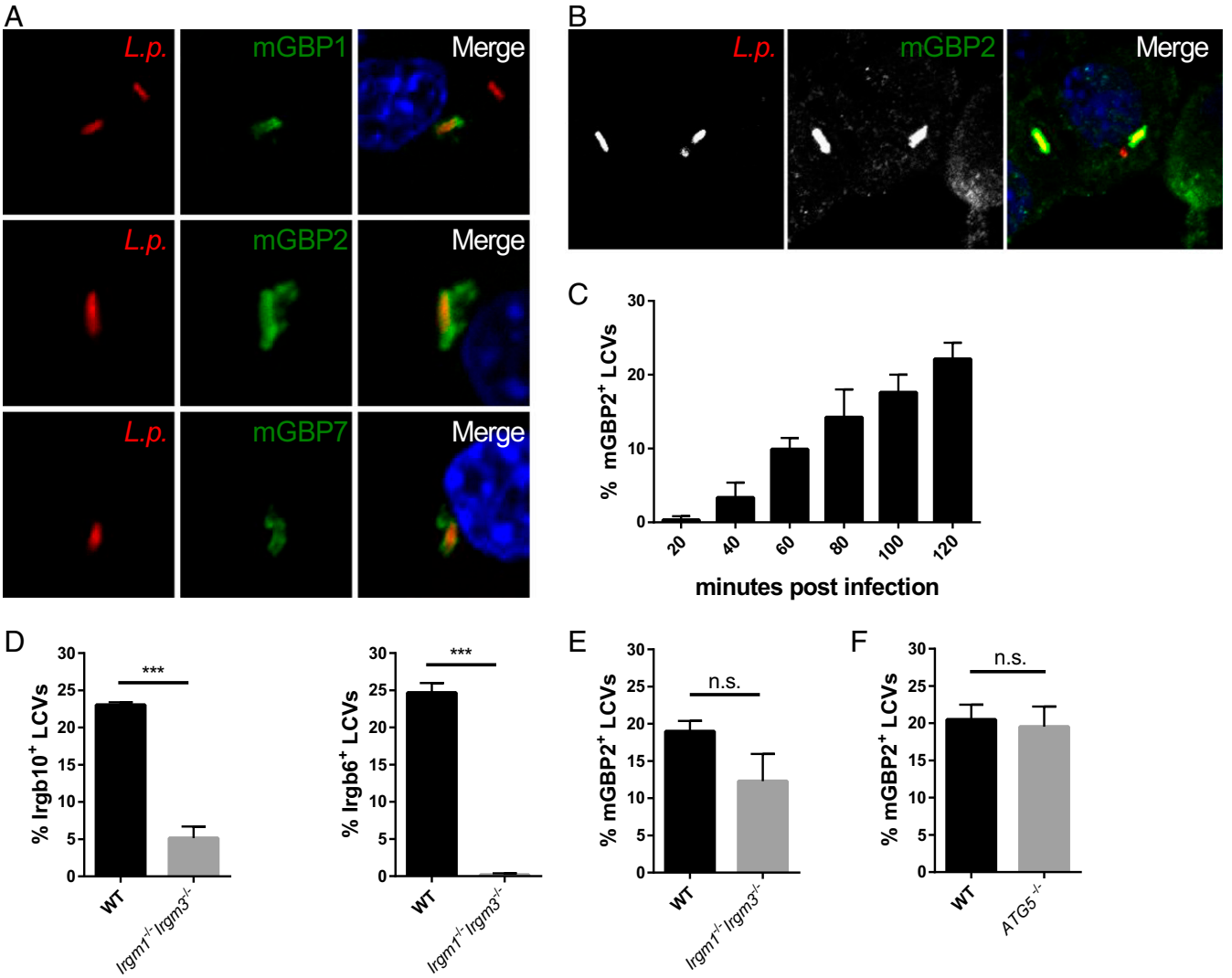

Fig. 1. GBPs associate with LCVs independent of IRGs and ATG5. Confocal images of dsRED$^+$ *L. pneumophila* (*L.p.*)-infected RAW 264.7 macrophages expressing GFP-mGBP1, GFP-mGBP2, or GFP-mGBP7 (*A*) and confocal images of IFN-γ–primed, *L. pneumophila*-infected BMDMs stained with anti-mGBP2 antibody at 2 hpi (*B*) are shown. Percentages of mGBP2$^+$ LCVs in IFN-γ–primed BMDMs were quantified in 20-min intervals for the first 2 hpi (*C*). Frequencies of Irgb10$^+$ and Irga6$^+$ LCVs in IFN-γ–primed WT vs. *Irgm1*$^{-/-}$*Irgm3*$^{-/-}$ BMDMs at 2 hpi are shown (*D*). Frequencies of mGBP2$^+$ LCVs in IFN-γ–primed WT vs. *Irgm1*$^{-/-}$*Irgm3*$^{-/-}$ (*E*) or *ATG5*$^{-/-}$ BMDMs (*F*) are shown. Error bars represent SDs. At least three independent experiments were performed. Statistical analysis was performed by unpaired two-tailed Student's *t* test (***$P < 0.005$; n.s., not significant). (Magnification, 63×.)

was necessary and sufficient to trigger mGBP2 delivery to vacuoles. The T3SS of *Y. pseudotuberculosis* secretes a small number of effector proteins, which includes the antiphagocytic factor YopE (37). Therefore, WT *Y. pseudotuberculosis* can block phagocytosis by macrophages. To allow macrophages to ingest *Y. pseudotuberculosis* and to test whether secreted effectors are required for the recruitment of mGBP2 to PVs, we exposed IFN-γ–primed BMDMs to the "effectorless" *Y. pseudotuberculosis* Δ*HOJMEK* mutant strain (38), which lacks all known translocated effector proteins including YopE. At 2 hpi, approximately 15% of all YCVs formed by ΔHOJMEK stained mGBP2-positive (Fig. 2*C*), demonstrating that the secretion of T3SS effector proteins is not necessary to trigger mGBP2 recruitment to YCVs.

We next asked whether the presence of the bacterial secretion system itself could be detected by GBPs. The T3SS system consists of structural proteins forming the base, the inner rod, and the needle. This part of the apparatus enables Gram-negative bacteria to secrete effectors across the inner and outer membranes of the bacterial cell wall. The delivery of effectors into the host cell cytosol by extracellular or vacuolar pathogens requires an additional bacterial translocon complex, which is inserted into host cell membranes (39). We hypothesized that GBPs could sense the insertion of such a bacterial pore complex into PV membranes. In *Y. pseudotuberculosis*, the T3SS translocon complex is made of the two proteins YopB and YopD (39). To test our hypothesis that the host detects the YopB/YopD translocon complex, we monitored recruitment of mGBP2 to vacuoles containing the effectorless *Y. pseudotuberculosis* strain with an additional deletion in *yopD* (Δ*DHOJMEK*). Deletion of *yopD* largely abrogated the delivery of mGBP2 to YCV (Fig. 2*C*), indicating that the presence of the YopB/YopD translocon complex is necessary for the delivery of mGBP2 to YCVs.

The secretion of Yop proteins is tightly controlled by the effector YopK. YopK-deficient strains release more translocon proteins than YopK-competent strains (40–42). We therefore hypothesized that YopK would be able to block mGBP2 recruitment to YCVs, if mGBP2 was indeed able to detect the

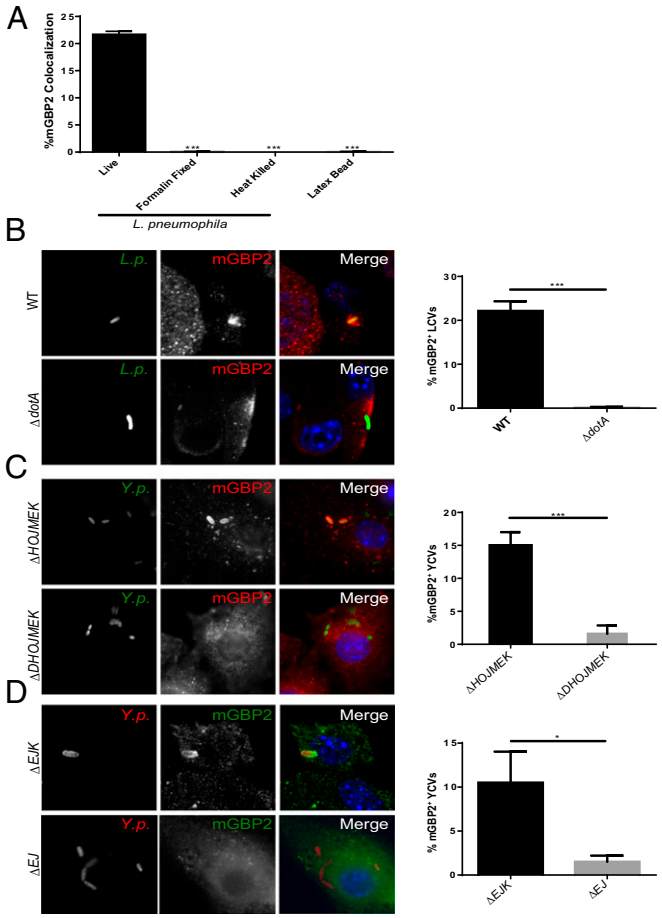

Fig. 2. mGBP2 targets vacuoles containing live bacteria expressing bacterial secretion systems. Live or dead dsRED$^+$ *L. pneumophila* (L.p.) or latex beads were fed to IFN-γ–primed BMDMs for 2 h. The percentages of mGBP2-positive phagocytosed bacteria or beads are depicted (*A*). IFN-γ–primed BMDMs were infected with GFP$^+$ *L. pneumophila* (*B*), GFP$^+$ *Y. pseudotuberculosis* (Y.p.) (*C*), or mCherry$^+$ *Y. pseudotuberculosis* (*D*) of the indicated genotypes. Representative images and percentages of mGBP2$^+$ PVs at 2 hpi are shown. A minimum of 200 infected cells was analyzed per condition and experiment. At least three independent experiments were performed. Error bars represent SDs. Statistical analysis was performed by one-way ANOVA with Tukey's multiple comparison test (*A*) and unpaired two-tailed Student's *t* test (*B–D*; $*P < 0.05$ and $***P < 0.005$). (Magnification, 63×.)

presence of translocon proteins in YCV membranes. To test our hypothesis, we compared mGBP2 recruitment to YCVs occupied by Δ*EJ* or Δ*EJK*, respectively. We used strains with a Δ*EJ* genetic background to permit phagocytosis and to avoid YopJ-mediated cell death (43, 44). We found that vacuoles harboring the YopK-deficient strain Δ*EJK* were decorated with mGBP2 at a higher frequency than the coisogenic control strain Δ*EJ* (Fig. 2*D*), demonstrating that YopK can protect YCVs against immune detection by mGBP2. Collectively, these data indicated that the host delivers mGBP2 to vacuolar membranes that contain components of bacterial secretion systems.

mGBP2 Colocalizes with Galectin-3 at Vacuoles Containing Bacteria Expressing Functional T3SS or T4SS. Several cytosolically localized members of the Galectin protein family were shown to associate with PVs formed by *S. enterica* or *L. pneumophila* (7, 10). Sporadic loss of membrane integrity in PVs is thought to be the underlying reason for the association of Galectins with PVs, but the molecular cause for the inherent instability of PV membranes remains enigmatic (5). We asked whether the presence of bacterial secretion systems could contribute to PV instability. To test this hypothesis, we monitored the subcellular localization of ectopically expressed YFP-Galectin-3 fusion protein in IFN-γ–primed, immortalized BMDMs (iBMDMs). As reported previously (7, 13), we observed that a sizeable percentage of WT LCVs attracted Galectin-3 (Fig. 3*A*). We found that Galectin-3 failed to colocalize with vacuoles containing the Δ*dotA* mutant, suggesting that the presence of the Dot/Icm T4SS apparatus contributes to diminished LCV integrity.

The relative instability of WT LCVs compared with Δ*dotA* vacuoles could result from the effects of vacuolar remodeling by secreted effector proteins or the insertion of a bacterial secretion system into LCV membranes. Distinguishing between these two competing models is difficult, as *L. pneumophila* secretes hundreds of effector proteins and an effectorless *L. pneumophila* mutant strain is unavailable (35). We therefore pursued an alternative approach by assessing the colocalization of Galectin-3 with vacuoles containing Δ*EJK* or Δ*EJ* mutant *Y. pseudotuberculosis* strains, which differ in their secretion and assembly of the translocon complex (42). We observed a substantial increase in Galectin-3–positive vacuoles containing the Δ*EJK* strain, which secretes excess amounts of the pore-forming proteins YopB and YopD. These results suggested that the insertion of translocon proteins into YCV membranes is the underlying cause for vacuolar instability (Fig. 3*B*).

Galectin-3 and mGBP2 associated with LCVs or YCVs at comparable frequencies (Figs. 2 and 3), suggesting that these two proteins target the same subset of LCVs and YCVs. In support of this hypothesis, we observed colocalization of mGBP2 and YFP–Galectin-3 at LCVs (Fig. 4*A*) and at YCVs (Fig. 4*B*) in IFN-γ–primed BMDMs. The majority of Galectin-3–decorated LCVs and YCVs also stained positive for mGBP2 and vice versa (Fig. 4 *C* and *D*). As expected, Δ*dotA* LCVs were devoid of detectable Galectin-3/mGBP2 costaining, and only a small percentage of Δ*EJ* vacuoles were decorated with either host protein (Fig. 4 *C* and *D*). Together, these data demonstrated that the presence of the *Legionella* T4SS or hypersecretion of *Yersinia*

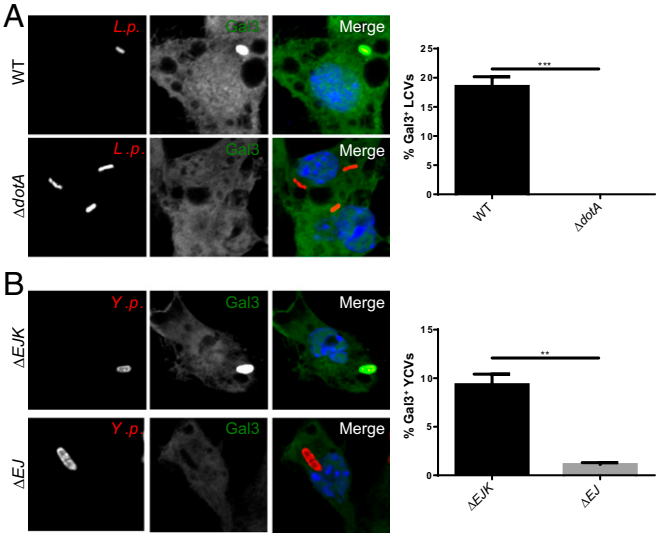

Fig. 3. Galectin-3 colocalizes with dotA-expressing *L. pneumophila* (L.p.) and YopB-/YopD-hypersecreting *Y. pseudotuberculosis*. (Y.p.) YFP-Gal3–expressing iBMDMs were infected with dsRED$^+$ *L. pneumophila* (*A*) or mCherry$^+$ *Y. pseudotuberculosis* (*B*) of the indicated genotypes. The percentage of Gal3$^+$ PVs at 2 hpi is depicted. A minimum of 200 infected cells were quantified per condition and experiment. At least three independent experiments were performed. Error bars represent SDs. Statistical analysis was performed by two-tailed Student's *t* test ($**P < 0.01$ and $***P < 0.005$). (Magnification, 63×.)

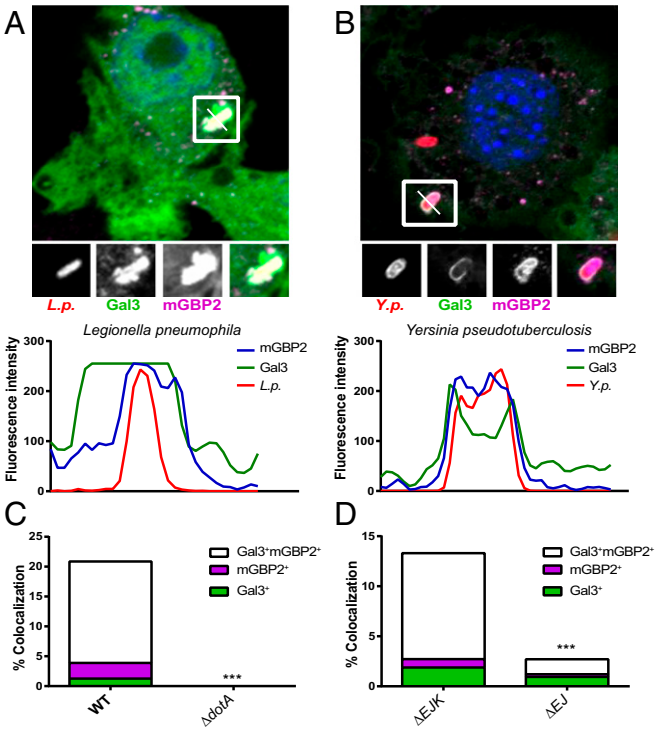

Fig. 4. Galectin-3 and mGBP2 colocalize at PVs. YFP-Gal3–expressing iBMDMs were infected with dsRED$^+$ WT *L. pneumophila* (L.p.) (*A*) or mCherry$^+$ WT *Y. pseudotuberculosis* (Y.p.) (*B*) and stained for endogenous mGBP2 at 2 hpi. Representative colocalization analysis and line trace are shown. The percentage of LCVs (*C*) or YCVs (*D*) staining positive for Galectin-3 only, mGBP2 only, or dual-positive for Galectin-3 and mGBP2 are shown. A minimum of 100 infected cells were quantified per condition and experiment. At least three independent experiments were performed. Statistical analysis by two-tailed student's *t* test for double-positive bacteria is shown (***$P < 0.005$). (Magnification, 63×.)

T3SS translocon proteins promote the concomitant recruitment of Galectin-3 and mGBP2 to PVs.

Mouse and Human GBPs Colocalize with Galectin-3 at Sterilely Damaged Host Vesicles. Galectins bind to glycosylated proteins residing extracellularly or on the luminal face of intracellular vesicles. Ruptured vesicles expose glycosylated proteins to the host cell cytosol and thereby recruit Galectins. Because mGBP2 and Galectin-3 colocalize at LCVs and YCVs (Fig. 4), we asked whether mGBP2 and Galectin-3 could also be corecruited to sterilely damaged vesicles. To test our hypothesis, we induced damaged vesicles by hypotonic shock. As expected, cells exposed to hypotonic shock conditions accumulated Galectin-3 puncta, which is indicative of the formation of damaged vesicles (Fig. 5*A* and Fig. S3). Similarly, we observed an accumulation of mGBP2 puncta in IFN-γ–primed BMDMs exposed to hypotonic shock (Fig. 5*A* and Fig. S3) and found that approximately 20% of all Galectin-3 puncta formed in these cells also stained positive for mGBP2 (Fig. 5*A*). Next, we exposed mouse embryonic fibroblasts (MEFs) to calcium phosphate precipitates (CPPs) known to cause endosomal damage and to recruit Galectin-3 (45). We observed that more than half of all CPP-damaged, Galectin-3–positive endosomes acquired mGBP2 in IFN-γ–primed MEFs (Fig. 5*B*). As a third method to sterilely induce vesicular damage, we exposed IFN-γ–primed BMDMs to the lysosomotropic compound L-Leucyl-L-leucine methyl ester (LLOMe), which disrupts lysosomal membranes (46). LLOMe treatment induced the formation of Galectin-3–positive structures, of which approximately half also stained positive for mGBP2 (Fig. 5*C*). Together, these data demonstrated that mGBP2 was recruited to multiple types of damaged vesicles.

GBPs constitute relatively large protein families in rodents and primates, with 11 murine and 7 human family members (16). We next asked whether the ability of mGBP2 to detect damaged vesicles was conserved in any of the human GBP orthologs. To address this question, we individually expressed mCherry-hGBP1-7 fusion proteins in human embryonic kidney (HEK) 293T cells that also expressed YFP–Galectin-3. We then induced vesicular damage by CPP or LLOMe treatment and found that hGBP1 colocalized with ∼60% of Galectin-3 puncta in CPP-treated HEK 293T cells and 35% of Galectin-3 puncta in LLOMe-treated HEK 293T cells (Fig. 5*D*). With the exception of a few colocalization events between hGBP2 and Galectin-3, we failed to detect recruitment of any of the other ectopically expressed human GBP paralogs to damaged vesicles in 293T cells (Fig. 5*D*). Collectively, these data showed that the targeting of GBPs to damaged vesicles is conserved from mice to humans.

Galectin-3 and mGBP2 Form Protein Complexes. Because Galectin-3 and mGBP2 colocalized at damaged vesicles and at PVs, we asked whether these proteins would also physically interact. To address this question, we used GFP-Trap immunoprecipitations (IPs) in IFN-γ–primed iBMDMs transduced with an YFP–Galectin-3 expression construct. GFP-Trap beads efficiently immunoprecipitated YFP–Galectin-3 and coimmunoprecipitated endogenous mGBP2 from LLOMe-treated iBMDMs, and, to a lesser degree, from untreated iBMDMs (Fig. 6*A*). As expected,

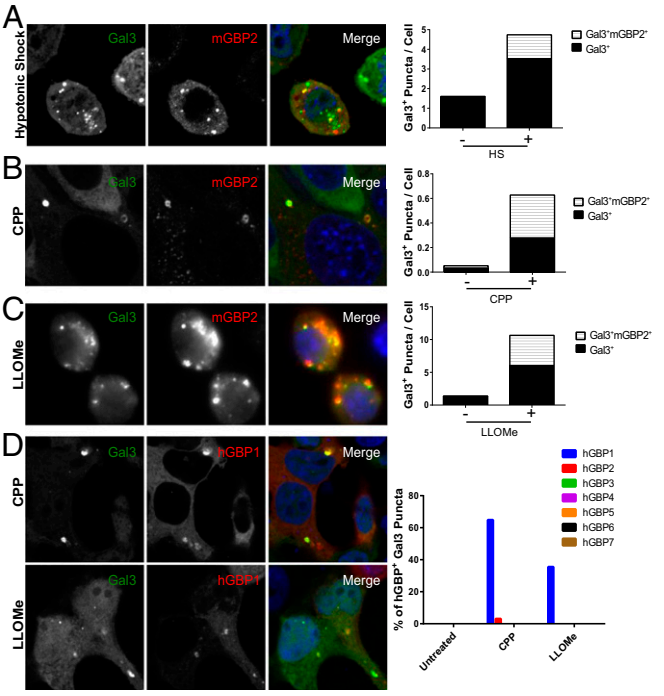

Fig. 5. Galectin-3 and GBPs colocalize at sterilely damaged vesicles. YFP-Gal3–expressing iBMDMs were exposed to hypotonic shock, and the formation of Gal3$^+$ puncta and the frequency of their colocalization with mGBP2 are shown (*A*). Endosomal damage in MEFs expressing YFP-Gal3 was induced by CPP treatment, and the quantification of Gal3$^+$ puncta and colocalization with mGBP2 are shown by treatment (*B*). YFP-Gal3–expressing iBMDMs were damaged with LLOMe, and the formation of Gal3$^+$ puncta and colocalization with mGBP2 were quantified (*C*). HEK 293T cells expressing YFP-Gal3 and hGBP-mCherry fusion proteins were treated with CPP or LLOMe. The percentages of YFP-Gal3 puncta colocalizing with individual hGBP orthologs are shown (*D*). A minimum of100 damaged cells were quantified per condition and experiment. HS, hypotonic shock. (Magnification, 63×.)

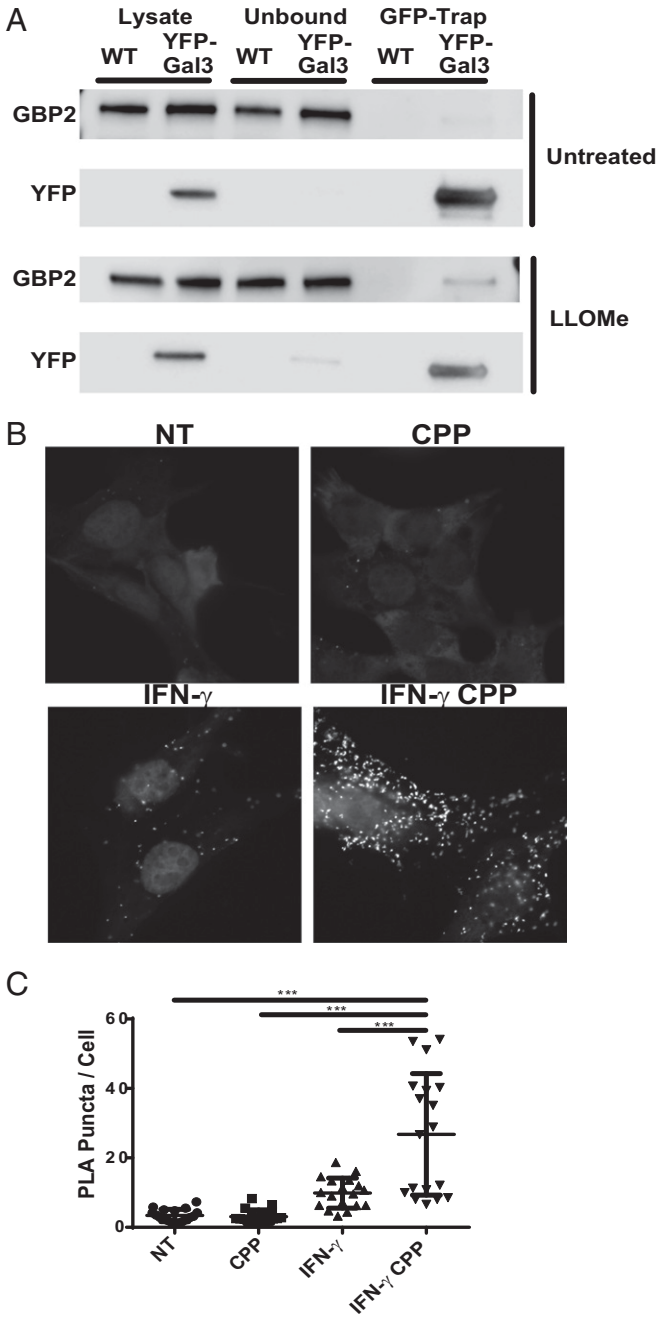

Fig. 6. Galectin-3 and mGBP2 form protein complexes. iBMDMs transduced with YFP-Gal3 retrovirus or untransduced controls were damaged with LLOMe or left untreated, and the formation of GBP2/YFP-Gal3–containing protein complexes was assessed with by GFP-Trap IPs. Whole-cell lysates and unbound and IP fractions were immunoblotted against GBP2 and YFP (*A*). IFN-γ–primed and unprimed MEFs expressing YFP-Gal3 were treated with CPP or left untreated, and interaction was detected by PLA and quantified. A minimum of 15 fields were quantified per treatment. Represenative images (*B*) and quantification (*C*) are shown. At least three independent experiments were performed. Statistical analysis was performed by two-way ANOVA with Tukey's multiple comparison test (***$P < 0.005$). NT, nontreated. (Magnification, 63×.)

GFP-Trap beads failed to coimmunoprecipitate endogenous mGBP2 in untransduced control iBMDMs (Fig. 6*A*). As an independent approach, we performed proximity ligation assays (PLAs) in YFP-Galectin-3–expressing MEFs. Using antibodies directed against YFP and mGBP2, we detected a significant increase in PLA puncta in IFN-γ–primed cells treated with CPP (Fig. 6*B*). Collectively, these data demonstrated that Galectin-3 and mGBP2 form protein complexes in response to vesicular damage.

Galectin-3 Promotes the Recruitment of mGBP2 and p62 to PVs. Because Galectin-3 and mGBP2 form protein complexes that localize to PVs, we asked whether Galectin-3 or other members of the Galectin family could control the recruitment of mGBP2 to PVs. To test this hypothesis, we first screened a set of YFP-Galectin expression constructs for colocalization with LCVs. We found that Galectin-8 and Galectin-9, in addition to Galectin-3, associated with LCVs in iBMDMs (Fig. 7*A*). To determine whether LCV-resident Galectins played a role in the delivery of mGBP2 to LCVs, we interfered with the expression of individual LCV-associated Galectins by using shRNAs. We observed a reduced percentage of mGBP2-positive LCVs in IFN-γ–primed iBMDMs that expressed Galectin-3 shRNAs or, albeit to a lesser extent, Galectin-8 shRNAs (Fig. 7*B*). To independently interrogate the function of Galectin-3 in directing mGBP2 to PVs, we monitored the subcellular localization of mGBP2 in BMDM derived from Galectin-3–deficient (*Gal3*$^{-/-}$) mice. As expected, *Gal3*$^{-/-}$ and WT BMDMs expressed comparable levels mGBP2 protein under IFN-γ priming conditions (Fig. S4). Nonetheless, recruitment of endogenous mGBP2 to LCVs (Fig. 7*C*) or YCVs (Fig. 7*D*) was significantly reduced in IFN-γ–primed *Gal3*$^{-/-}$ relative to WT BMDM. Ectopically expressed GFP-mGBP1 or GFP-mGBP2 also displayed reduced colocalization with YCVs in *Gal3*$^{-/-}$ iBMDM (Fig. 7*E*). Because Galectin-8–mediated recruitment of NDP52 to SCVs is dependent on the recognition of intravacuolar host glycans (10), we asked whether recruitment of mGBP2 to PVs was regulated in a similar fashion. To answer this question, we treated RAW 264.7 cells with the O-glycosylation inhibitor benzyl-GalNAc (BGN) before infection with *Y. pseudotuberculosis*. We found that BGN treatment significantly reduced the association of mGBP2 with Δ*EJK* (Fig. 7*F*) or Δ*HOJMEK* vacuoles (Fig. S5), suggesting that Galectin-3–mediated recruitment of mGBP2 to YCVs requires recognition of host glycans.

We next monitored the localization of the mGBP1-interacting protein p62 to YCVs. We observed a decrease in the percentage of p62-positive YCVs in GBP-deficient (*GBP*$^{chr3-/-}$) and, to a lesser degree, in *Gal3*$^{-/-}$ BMDMs (Fig. 7*H*). This decrease in p62 recruitment correlated with a similar decrease in the number of ubiquitin-decorated YCVs in *GBP*$^{chr3-/-}$ and *Gal3*$^{-/-}$ BMDMs (Fig. 7*I*), indicating that GBPs recruit the ubiquitin-binding protein p62 to PVs directly or, alternatively, indirectly through the activation of a PV-targeted ubiquitination pathway. Because the number of ubiquitin-positive YCVs was only partially reduced in *GBP*$^{chr3-/-}$ BMDMs, we tested whether GBP-independent YCV ubiquitination pathways existed. We previously demonstrated an essential role for the IRG proteins Irgm1 and Irgm3 in the ubiquitination of *C. trachomatis* PVs in mouse cells (21). Here, we found that the absence of Irgm1 and Irgm3 partially reduced the number of ubiquitin-decorated YCVs (Fig. S6), suggesting that IRGs and GBPs control parallel pathways of PV recognition and ubiquitination. In agreement with a model in which IRGs and Galectin-3/GBPs control parallel, functionally redundant pathways of YCV and LCV recognition, we found IFN-γ–primed *Gal3*$^{-/-}$ BMDMs to restrict bacterial growth, similar to WT BMDMs (Fig. S7). Together, our findings demonstrate that Galectin-3 promotes the recruitment of mGBP2 to LCVs and YCVs in a host glycan-dependent manner as part of a complex network of PV recognition pathways.

Discussion

IFN-inducible GBPs provide cell-autonomous immunity to intracellular pathogens residing within customized PVs. Although it has been shown that GBPs translocate to PVs and kill PV-resident

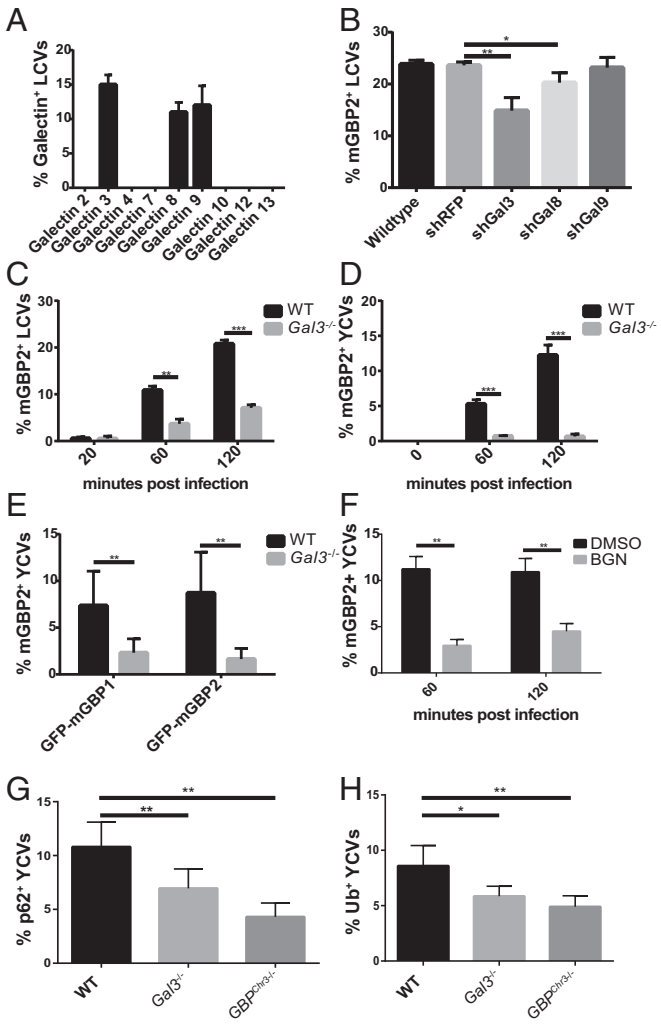

Fig. 7. Galectin-3 promotes targeting of mGBP2 and p62 to LCVs and YCVs. WT iBMDM expressing individual Galectins as YFP-fusion proteins were infected with dsRED$^+$ *L. pneumophila*. The percentages of Galectin$^+$ LCVs were quantified at 2 hpi (*A*). WT iBMDMs were treated with shRNA against Galectin-3, -8, and -9, and the percentages of mGBP2$^+$ LCVs were quantified at 2 hpi (*B*). WT and *Gal3*$^{-/-}$ BMDMs were infected with dsRED$^+$ *L. pneumophila* (*C*) or mCherry$^+$ Δ*EJK Y. pseudotuberculosis* (*D*), and the percentages of mGBP2$^+$ PVs were quantified over time. Colocalization of GFP-mGBP1 and GFP-mGBP2 with Δ*EJK* YCVs was monitored in WT and *Gal3*$^{-/-}$ iBMDMs at 2 hpi (*E*). RAW 264.7 cells were treated with 2 mM BGN or DMSO control for 3 d before infection with *Y. pseudotuberculosis* Δ*EJK*. Percentages of mGBP2$^+$ YCVs were quantified at the indicated time points (*F*). BMDMs of the indicated genotypes were infected with Δ*EJK*, and YCV colocalization with p62 (*G*) or ubiquitin (*H*) was assessed at 2 hpi. A minimum of 100 infected cells were counted per experimental condition and experiment. At least three independent experiments were performed except for the experiment shown in *A*, which was repeated once. Error bars represent SDs. Statistical analysis was performed by two-way ANOVA (*B*, *G*, and *H*), two-tailed Student's *t* test (*C*, *D*, and *E*), and one-way ANOVA with Tukey's multiple comparison test (*F*; $*P < 0.05$, $**P < 0.01$, and $***P < 0.005$).

microbes, the mechanisms by which GBPs specifically identify and bind to PVs are largely unknown (16). Here, we demonstrate that vacuolar disruption mediated by bacterial secretion apparatuses provides a pattern of pathogenesis, which prompts the delivery of antimicrobial GBPs to PVs.

To combat infections with PV-resident pathogens, the host must be able to discriminate between "nonself" PV membranes and endomembranes. To do so, a subset of "membrane-surveying" PRRs are predicted to detect patterns that are unique to PV membranes (25). One such pattern is provided by the occasional compromise of PV membrane integrity. Although pathogens such as *S. enterica* and *Mycobacterium tuberculosis* are traditionally classified as vacuolar pathogens, a proportion of these bacteria exits PVs and replicates inside the host cell cytosol (47, 48). The host cell can detect the breakdown of these PVs and activate host resistance mechanisms (49). The rupture of *Mycobacterium*-containing vacuoles (MCVs) by the bacterial ESX-1 virulence system, for example, triggers the recruitment of the host ubiquitin E3 ligase parkin to MCVs, leading to MCV ubiquitination and subsequent targeting and degradation of bacteria within autophagosomes (50).

Although active egress from PVs is occasionally executed by vacuolar pathogens as a strategy to promote intracellular replication, loss of membrane integrity may also occur as an unintended consequence of PV manipulations by resident bacteria (5). Previous studies have demonstrated that PV membrane remodeling and manipulations of PV trafficking by secreted effector proteins can stabilize and destabilize PV membranes (7–9). The present study shows that hypersecretion of *Yersinia* YopB/YopD pore proteins is sufficient to recruit the vacuolar damage sensor Galectin-3 to YCVs independent of the secretion of bacterial effectors. Thus, our work suggests that the insertion of bacterial translocation pores into PV membranes is in itself a pattern of pathogenesis that can be detected by the innate immune system. The tight control over the secretion of bacterial pore complexes, as illustrated by the function of YopK in limiting the translocation of YopB and YopD (40, 41), is therefore likely designed as a microbial stealth strategy to avoid immune detection (51, 52).

Loss of vacuolar integrity renders the luminal side of PVs accessible to the host cell cytosol. As a consequence of increased PV membrane permeability, cytosolic Galectins bind to glycans confined to the PV interior (11). The disintegration of PVs attracts Galectin-3, -8, and -9, but only the functional consequences of Galectin-8 recruitment to PVs was previously reported (10). Here, we describe a function for Galectins in regulating the delivery of GBPs to PVs. We demonstrate that Galectin-3 and mGBP2 form a protein complex and that Galectin-3 facilitates the targeting of mGBP2 to PVs. Galectin-8 appears to also promote the delivery of mGBP2 to PVs, albeit less efficiently. Galectin-8–mediated delivery of mGBP2 to YCVs or LCVs likely explains the rare occurrence of mGBP2-positive but Galectin-3–negative PVs (Fig. 4). Similar to previous observations (10), our data suggest that host cells detect ruptured PVs as a result of the cytosolic exposure of intravacuolar host glycans. We demonstrate that inhibition of host O-glycosylation reduces the recruitment of mGBP2 to YCVs, but not in full. Therefore, N-glycosylated host proteins or bacterial PAMPs associated with PV membranes could provide additional signals that direct Galectins and GBPs to PVs.

Galectin-mediated recognition of PVs is not the only pathway by which the host can deliver GBPs to PVs. We previously reported that IFN-γ priming triggers the ubiquitination of *Chlamydia* and *Toxoplasma* PVs and the ubiquitin-dependent recruitment of GBPs to these PVs (21). The ubiquitination of *Chlamydia* and *Toxoplasma* PVs and the subsequent recruitment of GBPs to PVs requires the IFN-γ–inducible GTPases Irgm1 and Irgm3 (20, 21). In the current study, we show that the association of GBPs with LCVs is independent of Irgm1 and Irgm3, demonstrating that GBPs can be delivered to PVs by Irgm-dependent and -independent pathways. It is currently unknown whether these two pathways mediate the translocation of all or only subsets of GBPs to PVs, whether additional GBP targeting pathways exist, and if and how pathogens interfere with Galectin-dependent attacks on PVs.

Finally, our study reveals an unexpected role for GBPs in mobilizing ubiquitin to PVs. GBPs are dispensable for the ubiquitination of *Chlamydia* or *Toxoplasma* PVs in mouse cells, a

process that instead requires Irgm1 and Irgm3 (21, 22). In human cells, on the contrary, ubiquitination of *Chlamydia* PVs is hIRGM-independent (53). Here, we show that Irgm-dependent and GBP-dependent pathways target ubiquitin to YCVs inside IFN-γ–primed mouse macrophages. Whether these two pathways are independent from one another or ultimately converge will need to be examined in the future. The possibility of functional redundancy between IRG- and GBP-mediated cell-autonomous immunity directed at PVs may explain why $GBP^{chr3-/-}$ and $Gal3^{-/-}$ BMDMs restrict intracellular growth of *L. pneumophila* or *Y. pseudotuberculosis*, similar to WT BMDMs (Fig. S7) (13). Alternatively, Galectin-3– and GBP-dependent PV ubiquitination may play regulatory roles, for example, in modulating cellular signaling that is initiated at PVs. Although a detailed understanding of the molecular and cellular activities of PV-resident GBPs remains elusive, the present study provides a vastly improved understanding of the mechanism by which GBPs identify and dock to PVs and thereby substantially advances the emerging field of GBP biology.

Materials and Methods

Cell Culture, Virus Production, Transduction, and Ectopic Gene Expression. BMDMs and MEFs were derived from the indicated mouse lines. WT (C57/BL6J) and $Gal3^{-/-}$ (54) mice were purchased from Jackson Laboratories. $GBP^{chr3-/-}$, $Irgm1^{-/-}Irgm3^{-/-}$, LysM-$Cre^{+}Atg5^{flox/flox}$, LysM-$Cre^{+}Atg7^{flox/flox}$, and LysM-$Cre^{+}Beclin^{flox/flox}$ mice were previously described (14, 23, 55). BMDMs were isolated from mouse femurs as described previously (13). Briefly, mouse bone marrow cells were cultured in BMDM media [RPMI 1640 + 20% (vol/vol) FBS + 12% (vol/vol) macrophage colony stimulating factor-conditioned media]. Immortalized iBMDMs were generated by culturing bone marrow cells in BMDM media and the presence of J2 virus as described previously (13). iBMDMs were grown for at least five passages after final virus treatment before experiments. MEFs were generated and cultured as described previously (28). Raw 264.7 and HEK 293T cells were obtained from the American Tissue Culture Collection (ATCC) and cultured according to ATCC recommendations. To deplete host glycans, Raw 264.7 cells were cultured for 3 d in the presence of 2 mM BGN. At 12 h before infection, cells were plated on poly-lysine–coated glass coverslips and primed with IFN-γ. Viral particles were produced in HEK 293T cells, and transduction was performed as described previously (20). At 48 h post transduction, cells were treated with puromycin or Blasticidin S (Invivogen), as appropriate for selection. The pLK0.1 lentiviral shRNA vectors TRCN0000301479, TRCN0000301480, and TRCN0000301477 (Gal3); TRCN0000066415, TRCN0000066416, and TRCN0000066417 (Gal8); and TRCN0000288518 and TRCN0000288440 (Gal9) were used to interfere with gene expression. More information on the constructs is available through the Broad Institute Web site (portals.broadinstitute.org/gpp/public/clone/search). M6P plasmids were used to produce recombinant murine leukemia virus (MLV) for the expression of YFP-tagged Galectin proteins in mammalian cells, as described previously (10). For increased transduction efficiency in iBMDMs, MLV particles were pseudotyped with vesicular stomatitis virus G protein. GFP-Gbp1, GFP-Gbp2, and GFP-Gbp7 were cloned in murine stem cell virus (MSCV) expression vectors by using standard procedures. MSCV transduction was performed as described previously (13). All seven human GBP paralogs were cloned into the expression vector pmCherry-C1 (Clontech) to generate fusion proteins with N-terminal mCherry tags. Constructs were transfected into HEK 293 cells to monitor subcellular localization of individual hGBP fusion proteins.

Bacterial Strains and Infections. All *L. pneumophila* experiments were conducted by using a flagellin-deficient LP01 strain (Δ*flaA*) (26) (annotated as WT) or a coisogenic Δ*flaA*Δ*dotA* strain (annotated as Δ*dotA*). Bacteria were grown in N-(2-Acetamido)-2-aminoethanesulfonic acid (ACES) buffered yeast extract broth at 37 °C overnight to reach postexponential phase. Infections were performed by using bacteria harvested from broth culture at an OD_{600} of 3.4–4. BMDMs were infected at a multiplicity of infection (MOI) of 1. Wt and Δ*dotA* coinfection experiments were not conducted at 4 °C as described previously (56), but at room temperature to render infections asynchronous. Bioluminescent *L. pneumophila* strains and growth assays were conducted as described previously (57). Luciferase readings were taken by using a Perkin–Elmer EnSpire plate reader. *Y. pseudotuberculosis* infections were carried out as follows. Bacteria were grown in 2× yeast extract tryptone broth overnight at 26 °C. Bacteria were then diluted into fresh media and supplemented with 20 mM sodium oxalate and 20 mM $MgCl_2$ for 1 h at 26 °C, followed by 2 h at 37 °C, before infection. Cells were infected with an MOI of 1 (Δ*EJ*, Δ*EJK*) or 0.5 (Δ*HOJMEK*, Δ*DHOJMEK*). Where indicated, cells were primed with murine IFN-γ (Millipore) at 100 U/mL overnight (12–16 h) before infection. All *Y. pseudotuberculosis* strains are coisogenic to IP2666. The strains Δ*EJ*, Δ*EJK*, and Δ*HOJMEK* were previously described (51, 52). To generate Δ*DHOJMEK,* an in-frame deletion in *YopD* was introduced in a Δ*HOJMEK* background. Strains were transformed with the GFP expression plasmid pFPV25.1 (Addgene) and mCherry expression plasmid pSS128, which constitutively expresses mCherry (generated and provided by the laboratory of Sunny Shin, University of Pennsylvania, Philadelphia).

Sterile Vesicle Damage. Endosomal damage by CPP was performed essentially as described before (45). Briefly, cells were plated on poly-D-lysine–treated coverslips. CPPs were prepared with equal volumes of $CaCl_2$ (256 mM) and buffer A (50 mM Hepes, 3 mM Na_2HPO_4, pH 7.05). CPPs were added dropwise to cells at 20% vol/vol and incubated for 4 h. Cells were fixed for 10 min in 4% (vol/vol) paraformaldehyde (PFA) and processed according to the standard immunofluorescence protocol. Hypotonic shock experiments were performed as described previously (10). Briefly, cells were incubated for 10 min in a solution of 10% (vol/vol) PEG 1,000 and 0.5 M sucrose, followed by two washes in PBS solution. They were then incubated in 60% (vol/vol) PBS solution in water for 3 min and returned to BMDM media for 20 min. Cells were then fixed for 10 min in 4% (wt/vol) PFA and processed for immunofluorescence. Lysosomal damage was induced by incubating cells with the lysosomotropic LLOMe at 1.5 mM for 2 h, except for the GFP-Trap experiments, in which LLOMe was used at 0.5 mM for 1 h.

Immunocytochemistry, PLAs, and Data Analysis. Cells were seeded onto glass coverslips in 24-well plates. Cells were treated as appropriate for the assay. Cells were fixed in 4% (wt/vol) PFA for 10 min at room temperature. Cells were then washed twice with PBS solution. For antibody staining, cells were permeabilized with 0.1% Triton X-100 for 15 min, blocked in 1% BSA supplemented with 0.3 M glycine for 30 min, and then incubated with primary antibodies for 1 h at room temperature. Subsequently, cells were incubated with secondary antibody at the appropriate dilution and treated with Hoechst 33258 to counterstain nuclei. Coverslips were then mounted to glass slides in a solution of Mowiol (Sigma) and 0.1% p-phenylenediamine (Sigma). Images were acquired on a Carl Zeiss Axio Observer.Z1 microscope or a Zeiss LSM 510 inverted confocal microscope. Colocalization and line trace analysis was performed with Fiji software (ImageJ; National Institutes of Health). To perform PLA, a Duolink In Situ Detection Kit (Sigma) was used following the manufacturer's recommended procedure for PLA probe dilutions and incubation times, rolling circle amplification times, and polymerase concentrations. For dual recognition of GBP2 and Gal3-YFP, the experiments were performed by using the anti-rabbit PLUS and anti-mouse MINUS secondary probes. Fluorescence image acquisition was performed on a Carl Zeiss Axio Observer.Z1 microscope or a Zeiss LSM 510 inverted confocal microscope. For all experiments, quantifications were performed from at least 10 images. High-resolution images from single scans were analyzed in Fiji to calculate the number of PLA puncta. Images were first smoothed, and a threshold was selected manually to discriminate PLA puncta from background fluorescence. When it had been selected, this threshold was applied uniformly to all images in the sample set. The built-in macro "Analyze Particles" was used to count and characterize all objects within images. The following primary antibodies and dilutions were used for immunofluorescence: rabbit polyclonal anti-Irgb10 at 1:1,000 (28), rabbit polyclonal anti-Irgb6 at 1:1,000 (19), rabbit polyclonal anti-GBP2 at 1:1,000 (20), mouse anti-Ubiquitin (FK2; Enzo) at 1:500, and rabbit anti-p62/SQSTM1 (MBL International) at 1:500. For PLA assays, mouse anti-GFP at 1:1,000 (Clontech) and rabbit anti-GBP2 1:2,000 were used.

GFP-Trap IP and Immunoblotting. To perform GFP-Trap IP, 5×10^6 YFP-Gal3–expressing iBMDMs or control iBMDMs were seeded in 10-cm untreated tissue culture dishes and then primed with 100 U/mL IFN-γ overnight or left unprimed. The following day, cells were treated with 0.5 mM LLOMe for 1 h. Cells were collected mechanically and spun at 600 × *g* for 5 min, resuspended, and washed twice in 1 mL PBS solution. Cells were incubated with 2 mM of the membrane-permeable cross-linker DSP (Thermo Scientific) for 30 min at room temperature. To stop the reaction, cells were incubated with 20 μM Tris, pH 7.5, for 15 min. The co-IP assay was performed with Chromotek GFP-Trap beads per manufacturer guidelines with slight modifications. To remove the cross-linking solution, cells were washed twice in cold PBS solution and lysed in 200 μL lysis buffer (10 mM Tris·HCl, pH 7.5, 150 mM NaCl, 0.5 mM EDTA, 0.5% Nonidet P-40) for 30 min on ice with vigorous pipetting every 10 min. The cell lysate was then spun at 20,000 × *g* for 10 min at 4 °C, and the supernatant was collected and diluted with 300 μL 4 °C dilution buffer (10 mM Tris·HCl, pH 7.5, 150 mM NaCl, 0.5 mM EDTA); 25 μL

was saved for lysate analysis. The diluted sample was mixed with washed GFP-Trap beads and incubated with end-over-end tumbling for 2 h at 4 °C. After incubation, 25 μL supernatant was saved for analysis (i.e., unbound), and the beads were washed three times in cold dilution buffer. To collect bead-bound proteins, the beads were resuspended in 50 μL 2× SDS sample buffer [120 mM Tris·Cl, pH 6.8, 20% (vol/vol) glycerol, 4% (wt/vol) SDS, 0.04% bromophenol blue, 10% (vol/vol) β-mercaptoethanol, and 20 mM DTT]. A total of 25 μL 2× SDS sample buffer was added to the 25 μL total lysate and unbound samples. SDS/PAGE was performed with BioRad 4–20% (wt/vol) precast Tris·glycine stain-free gels. Samples were run at 150 V for 45 min. Postelectrophoresis protein loading equivalency was checked by using a UV imager. Subsequently, the gel was transferred to nitrocellulose by using the BioRad semidry transfer apparatus. The transferred blot was blocked with 1% BSA for 30 min. Primary antibodies rabbit anti-Gbp2 (1:1,000) and mouse anti-eGFP (1:1,000) diluted in 1% BSA were incubated overnight at 4 °C. Blots were washed and incubated with secondary anti-rabbit and anti-mouse HRP antibodies for 30 min at room temperature. The membrane was activated with ECL (Perkin-Elmer/Western Lightning). Blots were developed on the Odyssey imaging system (LI-COR Biosciences).

Statistical Analysis. Where designated, statistical significance was determined by using the unpaired Student's *t* test or one- or two-way ANOVA as appropriate.

ACKNOWLEDGMENTS. We thank Dr. Gregory Taylor for sharing *Irgm1*$^{-/-}$ *Irgm3*$^{-/-}$ mouse bone marrow cells, Dr. Felix Randow for sharing YFP-Galectin expression constructs, Dr. Sunny Shin for sharing the mCherry expression plasmid, and Sarah Luoma for technical assistance. This work was supported by National Institutes of Health Grants R21AI122048 (to J.C.), R01AI103197 (to J.C.), and R01AI103062 (to I.E.B.), and Investigators in the Pathogenesis of Infectious Disease Awards from the Burroughs Wellcome Fund (to J.C. and I.E.B.).

1. Alix E, Mukherjee S, Roy CR (2011) Subversion of membrane transport pathways by vacuolar pathogens. *J Cell Biol* 195(6):943–952.
2. Juhas M, et al. (2009) Genomic islands: Tools of bacterial horizontal gene transfer and evolution. *FEMS Microbiol Rev* 33(2):376–393.
3. Zhao Y, Shao F (2015) The NAIP-NLRC4 inflammasome in innate immune detection of bacterial flagellin and type III secretion apparatus. *Immunol Rev* 265(1):85–102.
4. Vance RE, Isberg RR, Portnoy DA (2009) Patterns of pathogenesis: Discrimination of pathogenic and nonpathogenic microbes by the innate immune system. *Cell Host Microbe* 6(1):10–21.
5. Creasey EA, Isberg RR (2014) Maintenance of vacuole integrity by bacterial pathogens. *Curr Opin Microbiol* 17:46–52.
6. Lossi NS, Rolhion N, Magee AI, Boyle C, Holden DW (2008) The Salmonella SPI-2 effector SseJ exhibits eukaryotic activator-dependent phospholipase A and glycerophospholipid : Cholesterol acyltransferase activity. *Microbiology* 154(pt 9):2680–2688.
7. Creasey EA, Isberg RR (2012) The protein SdhA maintains the integrity of the Legionella-containing vacuole. *Proc Natl Acad Sci USA* 109(9):3481–3486.
8. Beuzón CR, et al. (2000) Salmonella maintains the integrity of its intracellular vacuole through the action of SifA. *EMBO J* 19(13):3235–3249.
9. Ruiz-Albert J, et al. (2002) Complementary activities of SseJ and SifA regulate dynamics of the Salmonella typhimurium vacuolar membrane. *Mol Microbiol* 44(3): 645–661.
10. Thurston TL, Wandel MP, von Muhlinen N, Foeglein A, Randow F (2012) Galectin 8 targets damaged vesicles for autophagy to defend cells against bacterial invasion. *Nature* 482(7385):414–418.
11. Chen HY, Weng IC, Hong MH, Liu FT (2014) Galectins as bacterial sensors in the host innate response. *Curr Opin Microbiol* 17:75–81.
12. Paz I, et al. (2010) Galectin-3, a marker for vacuole lysis by invasive pathogens. *Cell Microbiol* 12(4):530–544.
13. Pilla DM, et al. (2014) Guanylate binding proteins promote caspase-11-dependent pyroptosis in response to cytoplasmic LPS. *Proc Natl Acad Sci USA* 111(16):6046–6051.
14. Coers J, et al. (2011) Compensatory T cell responses in IRG-deficient mice prevent sustained Chlamydia trachomatis infections. *PLoS Pathog* 7(6):e1001346.
15. Borden EC, et al. (2007) Interferons at age 50: Past, current and future impact on biomedicine. *Nat Rev Drug Discov* 6(12):975–990.
16. Pilla-Moffett D, Barber MF, Taylor GA, Coers J (2016) Interferon-inducible GTPases in host resistance, inflammation and disease. *J Mol Biol* 428(17):3495–3513.
17. Kim BH, et al. (2016) Interferon-induced guanylate-binding proteins in inflammasome activation and host defense. *Nat Immunol* 17(5):481–489.
18. Man SM, et al. (2016) IRGB10 liberates bacterial ligands for sensing by the AIM2 and caspase-11-NLRP3 inflammasomes. *Cell* 167(2):382–396 e317.
19. Traver MK, et al. (2011) Immunity-related gtpase M (IRGM) proteins influence the localization of guanylate-binding protein 2 (GBP2) by modulating macroautophagy. *J Biol Chem* 286(35):30471–30480.
20. Haldar AK, et al. (2013) IRG and GBP host resistance factors target aberrant, "non-self" vacuoles characterized by the missing of "self" IRGM proteins. *PLoS Pathog* 9(6): e1003414.
21. Haldar AK, et al. (2015) Ubiquitin systems mark pathogen-containing vacuoles as targets for host defense by guanylate binding proteins. *Proc Natl Acad Sci USA* 112(41):E5628–E5637.
22. Lee Y, et al. (2015) p62 plays a specific role in interferon-γ-induced presentation of a toxoplasma vacuolar antigen. *Cell Reports* 13(2):223–233.
23. Yamamoto M, et al. (2012) A cluster of interferon-gamma-inducible p65 GTPases plays a critical role in host defense against Toxoplasma gondii. *Immunity* 37(2):302–13.
24. Kim BH, et al. (2011) A family of IFN-γ-inducible 65-kD GTPases protects against bacterial infection. *Science* 332(6030):717–721.
25. Coers J (2013) Self and non-self discrimination of intracellular membranes by the innate immune system. *PLoS Pathog* 9(9):e1003538.
26. Ren T, Zamboni DS, Roy CR, Dietrich WF, Vance RE (2006) Flagellin-deficient Legionella mutants evade caspase-1- and Naip5-mediated macrophage immunity. *PLoS Pathog* 2(3):e18.
27. Molofsky AB, et al. (2006) Cytosolic recognition of flagellin by mouse macrophages restricts Legionella pneumophila infection. *J Exp Med* 203(4):1093–1104.
28. Coers J, et al. (2008) Chlamydia muridarum evades growth restriction by the IFN-gamma-inducible host resistance factor Irgb10. *J Immunol* 180(9):6237–6245.
29. Khaminets A, et al. (2010) Coordinated loading of IRG resistance GTPases on to the Toxoplasma gondii parasitophorous vacuole. *Cell Microbiol* 12(7):939–961.
30. Choi J, et al. (2014) The parasitophorous vacuole membrane of Toxoplasma gondii is targeted for disruption by ubiquitin-like conjugation systems of autophagy. *Immunity* 40(6):924–935.
31. Ohshima J, et al. (2014) Role of mouse and human autophagy proteins in IFN-γ-induced cell-autonomous responses against Toxoplasma gondii. *J Immunol* 192(7): 3328–3335.
32. Haldar AK, Piro AS, Pilla DM, Yamamoto M, Coers J (2014) The E2-like conjugation enzyme Atg3 promotes binding of IRG and Gbp proteins to Chlamydia- and Toxoplasma-containing vacuoles and host resistance. *PLoS One* 9(1):e86684.
33. Selleck EM, et al. (2013) Guanylate-binding protein 1 (Gbp1) contributes to cell-autonomous immunity against Toxoplasma gondii. *PLoS Pathog* 9(4):e1003320.
34. Klionsky DJ, et al. (2016) Guidelines for the use and interpretation of assays for monitoring autophagy (3rd edition). *Autophagy* 12(1):1–222.
35. Isaac DT, Isberg R (2014) Master manipulators: An update on Legionella pneumophilaIcm/Dot translocated substrates and their host targets. *Future Microbiol* 9(3):343–359.
36. Finsel I, Hilbi H (2015) Formation of a pathogen vacuole according to Legionella pneumophila: How to kill one bird with many stones. *Cell Microbiol* 17(7):935–950.
37. Chung LK, Bliska JB (2016) Yersinia versus host immunity: How a pathogen evades or triggers a protective response. *Curr Opin Microbiol* 29:56–62.
38. Casson CN, et al. (2013) Caspase-11 activation in response to bacterial secretion systems that access the host cytosol. *PLoS Pathog* 9(6):e1003400.
39. Burkinshaw BJ, Strynadka NC (2014) Assembly and structure of the T3SS. *Biochim Biophys Acta* 1843(8):1649–1663.
40. Dewoody R, Merritt PM, Marketon MM (2013) YopK controls both rate and fidelity of Yop translocation. *Mol Microbiol* 87(2):301–317.
41. Francis MS, Wolf-Watz H (1998) YopD of Yersinia pseudotuberculosis is translocated into the cytosol of HeLa epithelial cells: Evidence of a structural domain necessary for translocation. *Mol Microbiol* 29(3):799–813.
42. Thorslund SE, et al. (2011) The RACK1 signaling scaffold protein selectively interacts with Yersinia pseudotuberculosis virulence function. *PLoS One* 6(2):e16784.
43. Monack DM, Mecsas J, Ghori N, Falkow S (1997) Yersinia signals macrophages to undergo apoptosis and YopJ is necessary for this cell death. *Proc Natl Acad Sci USA* 94(19):10385–10390.
44. Black DS, Bliska JB (2000) The RhoGAP activity of the Yersinia pseudotuberculosis cytotoxin YopE is required for antiphagocytic function and virulence. *Mol Microbiol* 37(3):515–527.
45. Chen X, et al. (2014) Autophagy induced by calcium phosphate precipitates targets damaged endosomes. *J Biol Chem* 289(16):11162–11174.
46. Maejima I, et al. (2013) Autophagy sequesters damaged lysosomes to control lysosomal biogenesis and kidney injury. *EMBO J* 32(17):2336–2347.
47. Knodler LA, et al. (2010) Dissemination of invasive Salmonella via bacterial-induced extrusion of mucosal epithelia. *Proc Natl Acad Sci USA* 107(41):17733–17738.
48. van der Wel N, et al. (2007) M. tuberculosis and M. leprae translocate from the phagolysosome to the cytosol in myeloid cells. *Cell* 129(7):1287–1298.
49. Boyle KB, Randow F (2013) The role of 'eat-me' signals and autophagy cargo receptors in innate immunity. *Curr Opin Microbiol* 16(3):339–348.
50. Manzanillo PS, et al. (2013) The ubiquitin ligase parkin mediates resistance to intracellular pathogens. *Nature* 501(7468):512–516.
51. Zwack EE, et al. (2015) Inflammasome activation in response to the Yersinia type III secretion system requires hyperinjection of translocon proteins YopB and YopD. *MBio* 6(1):e02095–e14.
52. Brodsky IE, et al. (2010) A Yersinia effector protein promotes virulence by preventing inflammasome recognition of the type III secretion system. *Cell Host Microbe* 7(5):376–387.
53. Haldar AK, et al. (2016) Chlamydia trachomatis is resistant to inclusion ubiquitination and associated host defense in gamma interferon-primed human epithelial cells. *MBio* 7(6):e01417-16.
54. Colnot C, Fowlis D, Ripoche MA, Bouchaert I, Poirier F (1998) Embryonic implantation in galectin 1/galectin 3 double mutant mice. *Dev Dyn* 211(4):306–313.
55. Martinez J, et al. (2015) Molecular characterization of LC3-associated phagocytosis reveals distinct roles for Rubicon, NOX2 and autophagy proteins. *Nat Cell Biol* 17(7):893–906.
56. Coers J, Monahan C, Roy CR (1999) Modulation of phagosome biogenesis by Legionella pneumophila creates an organelle permissive for intracellular growth. *Nat Cell Biol* 1(7):451–453.
57. Coers J, Vance RE, Fontana MF, Dietrich WF (2007) Restriction of Legionella pneumophila growth in macrophages requires the concerted action of cytokine and Naip5/Ipaf signalling pathways. *Cell Microbiol* 9(10):2344–2357.